

Attractor Dynamics in the Hippocampal Representation of the Local Environment

Tom J. Wills,¹ Colin Lever,¹ Francesca Cacucci,¹ Neil Burgess,^{1,2} John O'Keefe^{1*}

contribution to synapsis initiation as meiosis progresses.

Another function for centromere coupling might be the distributive disjunction system, which ensures the segregation of chromosomes that failed to cross over. Centromere regions in female flies have been shown to be important for distributive disjunction (16). In yeast, nonexchange chromosomes associate at their centromeres before segregation, and interfering with this association increases the rate of nondisjunction (17).

Centromeres appear to contribute to homolog alignment and segregation in other species as well, although the underlying mechanisms may be somewhat different. Nonhomologous centromere coupling is observed before homolog pairing during meiosis in wheat, but it is also observed in premeiotic tissues, arguing that centromere coupling does not depend on an SC protein (18, 19). In fission yeast, only centromeric regions are able to pair independently of meiotic recombination (20). The contributions of centromeres and SC proteins to homolog pairing in higher eukaryotes remain to be elucidated.

Memories are thought to be attractor states of neuronal representations, with the hippocampus a likely substrate for context-dependent episodic memories. However, such states have not been directly observed. For example, the hippocampal place cell representation of location was previously found to respond continuously to changes in environmental shape alone. We report that exposure to novel square and circular environments made of different materials creates attractor representations for both shapes: Place cells abruptly and simultaneously switch between representations as environmental shape changes incrementally. This enables study of attractor dynamics in a cognitive representation and may correspond to the formation of distinct contexts in context-dependent memory.

For more than 30 years, autoassociative or attractor dynamics based on Hebbian synaptic modification have been central to neuronal models of memory, with particular focus

on the dense recurrent collaterals of the hippocampus and its crucial role in context-dependent episodic memory (1–14). We investigated whether attractors were present in

References and Notes

- G. S. Roeder, *Genes Dev.* **11**, 2600 (1997).
- B. Rockmill, G. S. Roeder, *Genes Dev.* **12**, 2574 (1998).
- E. Trelles-Sticken, M. N. Conrad, M. E. Dresser, H. Scherthan, *J. Cell Biol.* **151**, 95 (2000).
- H. Dong, G. S. Roeder, *J. Cell Biol.* **148**, 417 (2000).
- S. Keeney, *Curr. Top. Dev. Biol.* **52**, 1 (2001).
- Materials and methods are available as supporting material on Science Online.
- K. A. Henderson, S. Keeney, *Proc. Natl. Acad. Sci. U.S.A.* **101**, 4519 (2004).
- P. R. Chua, G. S. Roeder, *Cell* **93**, 349 (1998).
- S. Agarwal, G. S. Roeder, *Cell* **102**, 245 (2000).
- T. Tsubouchi, G. S. Roeder, data not shown.
- J. C. Fung, B. Rockmill, M. Odell, G. S. Roeder, *Cell* **116**, 795 (2004).
- A. V. Smith, G. S. Roeder, *J. Cell Biol.* **136**, 957 (1997).
- K. M. Hyland, J. Kingsbury, D. Koshland, P. Hieter, *J. Cell Biol.* **145**, 15 (1999).
- A. F. Straight, A. S. Belmont, C. C. Robinett, A. W. Murray, *Curr. Biol.* **6**, 1599 (1996).
- D. K. Nag, H. Scherthan, B. Rockmill, J. Bhargava, G. S. Roeder, *Genetics* **141**, 75 (1995).
- M. Y. Walker, R. S. Hawley, *Chromosoma* **109**, 3 (2000).
- B. Kemp, R. M. Boumil, M. N. Stewart, D. S. Dawson, *Genes Dev.* **18**, 1946 (2004).
- B. Maestra, J. Hans de Jong, K. Shepherd, T. Naranjo, *Chromosome Res.* **10**, 655 (2002).
- E. Martinez-Perez, P. Shaw, G. Moore, *Nature* **411**, 204 (2001).
- D. Q. Ding, A. Yamamoto, T. Haraguchi, Y. Hiraoka, *Dev. Cell* **6**, 329 (2004).
- We thank members of the Roeder lab for helpful comments on the manuscript. T.T. thanks B. Rockmill and D. Dawson for helpful discussions and advice and is especially grateful to H. Tsubouchi for valuable insights. Supported by Ishizaka Foundation Scholarship (T.T.), NIH grant GM28904 (G.S.R.), and the Howard Hughes Medical Institute.

Supporting Online Material

www.sciencemag.org/cgi/content/full/308/5723/870/DC1

Materials and Methods

Fig. S1

References

6 December 2004; accepted 17 February 2005
10.1126/science.1108283

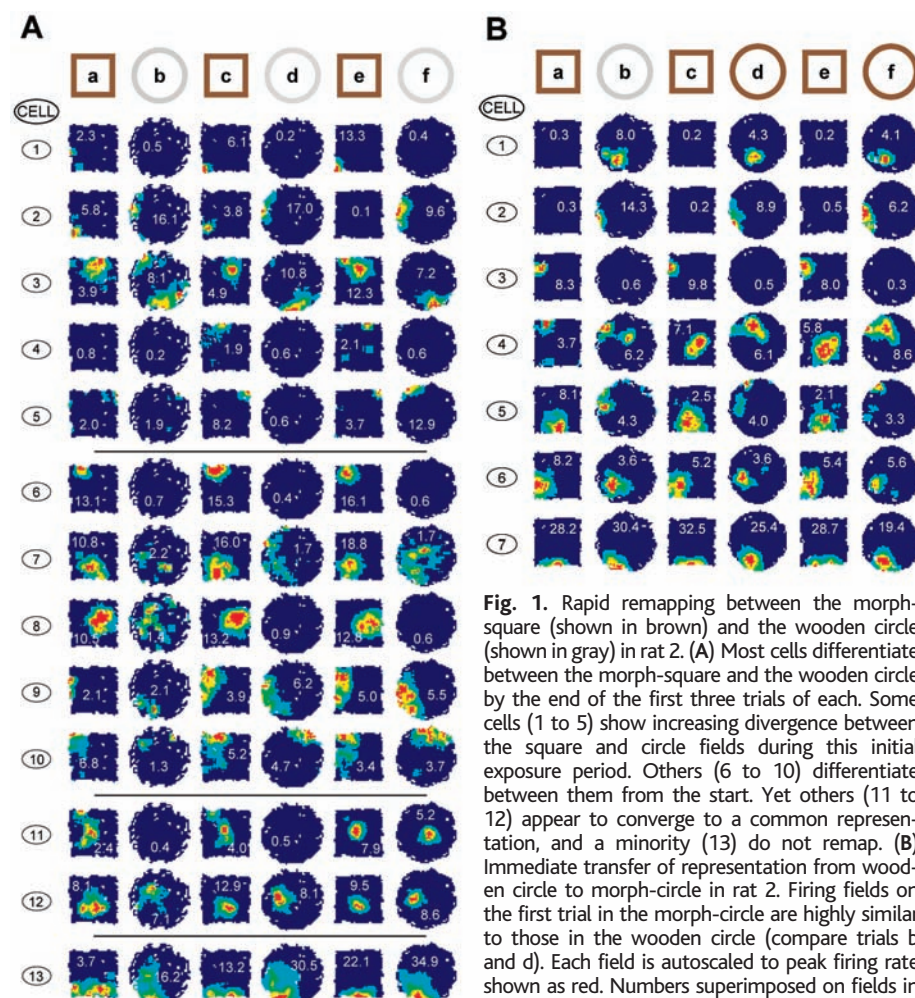


Fig. 1. Rapid remapping between the morph-square (shown in brown) and the wooden circle (shown in gray) in rat 2. (A) Most cells differentiate between the morph-square and the wooden circle by the end of the first three trials of each. Some cells (1 to 5) show increasing divergence between the square and circle fields during this initial exposure period. Others (6 to 10) differentiate between them from the start. Yet others (11 to 12) appear to converge to a common representation, and a minority (13) do not remap. (B) Immediate transfer of representation from wooden circle to morph-circle in rat 2. Firing fields on the first trial in the morph-circle are highly similar to those in the wooden circle (compare trials b and d). Each field is autocscaled to peak firing rate shown as red. Numbers superimposed on fields in this and subsequent figures show peak firing rates in Hz, to one decimal place.

the hippocampal representations of different environments.

Place cells in the mammalian hippocampus signal the location of the animal within its environment by firing whenever it visits a specific region [the “place field” (10, 15)]. This representation can be specific to the environment, with different cells being active in different environments or the same cell being active at different locations in different environments (16). The change in representation between environments is known as “remapping.” After foraging in square and circular boxes which differed only in their shapes (not texture or color), CA1 hippocampal place cells took considerable time (many days or weeks) to differentiate between the two boxes, with simultaneously recorded cells remapping at different times (17). Individual cells appeared to represent a location in one or both environments independently of other cells.

We recorded from CA1 place cells in a paradigm designed to produce more rapid remapping (18). Animals were initially exposed to a square and a circle that differed in color, texture, and shape. The square was a morph-box (17) (which can be configured in various shapes, see fig. S1, A and B); the circle was made of painted wood. This led to rapid remapping with the majority of cells (92%, that is, 48 out of 52) differentiating between the environments at the end of the first day’s six trials (three in each box, see Fig. 1A). After 3 days of this training, the animals were trained in the morph-box configured as a square and a circle on alternate trials for an additional 3 days (fig. S1C). The place fields of the majority of remapped cells (40 out of 46) transferred successfully to the morph-circle and showed the same pattern as in the wooden circle (see Fig. 1B). Different place fields in two configurations of the morph-box can only be cued by environmental shape, as other attributes such as texture and color do not vary. Of the six animals, one failed to show rapid remapping in the morph-square and wooden circle, and one did not show wooden circle to morph-circle pattern transfer. In these cases, the experiment was terminated. This paper describes results from the remaining four animals.

Are the different hippocampal representations of the morph-square and morph-circle after remapping due to the formation of separate attractors for each shape? If so, each representation would lie at the bottom of a “basin of attraction” within which other representations inevitably evolve into the

attractor representation under the system’s dynamics: Representations of intermediate shapes would revert to either the square or the circle representation (3, 6) (fig. S3, A to C). If not, representations of intermediate shapes would remain intermediate to those of the circle and square.

We recorded from groups of neurons during a series of probe trials in a set of octagonal morph-boxes (18) that varied from squarelike

(adjacent side ratio 1:7) to circlelike (adjacent side ratio 4:4) through more ambiguous intermediates (see Fig. 2 top row; fig. S1D). Almost all simultaneously recorded cells (28 out of 33) showed an abrupt switch from the squarelike pattern to the circlelike one across the octagonal series. The firing fields of 20 simultaneously recorded place cells in the series are shown in Fig. 2. Trials are presented in order of most squarelike on the left to most

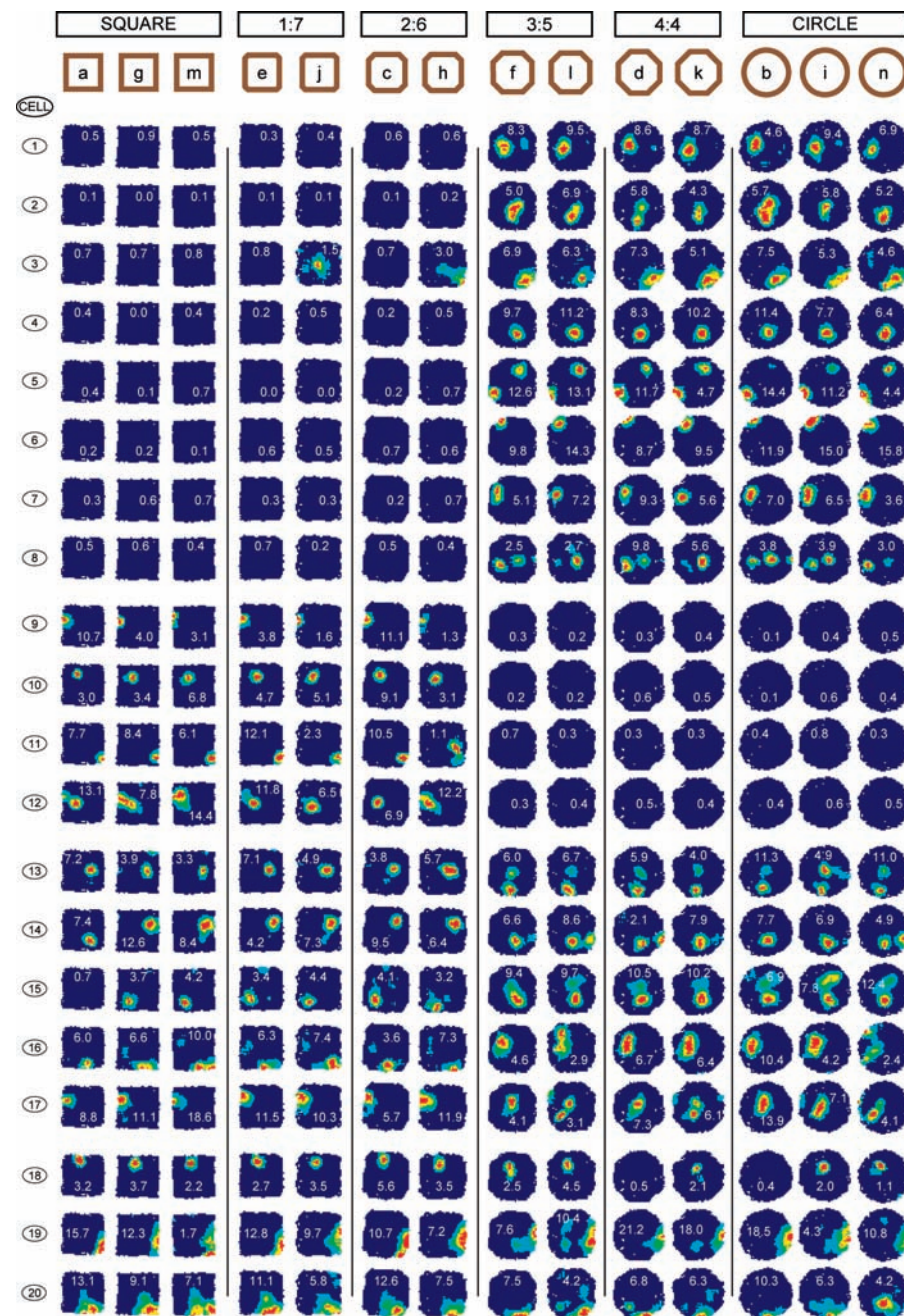


Fig. 2. Abrupt and coherent expression of squarelike or circlelike representation during probe trials in intermediate octagonal environments in rat 4. The 17 of 20 place cells simultaneously recorded from rat 4 with different (remapped) firing patterns in the square and the circle almost all switch from the squarelike to circlelike pattern between the 2:6 and 3:5 octagons. Eight cells had fields in the circle but not the square (cells 1 to 8); four in the square but not the circle (9 to 12); five fired in both but in different places (13 to 17); and three did not reach our criterion for remapping (18 to 20) (18).

¹Department of Anatomy and Developmental Biology, ²Institute of Cognitive Neuroscience, University College London, London WC1E 6BT, UK.

*To whom correspondence should be addressed. E-mail: j.keefe@ucl.ac.uk

circlelike on the right but were run in two series of interleaved and balanced order (fig. S1E). Seventeen of the 20 cells clearly remapped between the square and the circle: 12 remapped by changing rate (only firing in one or other shape), and 5 remapped their field position (firing in different places in the two shapes). The remaining three cells did not reach our criterion for remapping (18). Almost all of the cells abruptly switched from the squarelike to the circlelike pattern at the same transition point. This effect is quantified in Fig. 3A by comparing the similarity of each cell's firing in the octagons to that in the square and circle (18). A similar pattern was seen in the other three animals (Fig. 3, B to D left side).

The abrupt and coherent remapping of the place cell ensemble seems to require coordinated action, as in an autoassociative network, rather than to reflect cells independently

responding to the same subtle environmental changes. For example, if each cell independently remapped at any of the five shape transitions, the probability of N cells remapping at the same point would be 0.2^{N-1} ($P < 10^{-11}$ for the 17 cells from rat 4 in Fig. 2; $P < 10^{-4}$ for rat 1 in fig. S2A; $P < 0.05$ for rat 2 and rat 3, Fig. 3E and fig. S2B, respectively). This impression is strengthened by the remapping pattern in two of the four animals. In one animal (rat 2), the cells remapped between the 2:6 and 3:5 octagons during the first series of probe trials, but remapped between the square and 1:7 octagons during the second series (Fig. 3, C and E). Significantly, all cells again switched at the same point. Another animal (rat 3) showed a similar pattern, remapping at the 1:7 to 2:6 transition in the second series (Fig. 3D), whereas the remaining two animals remapped at the same point in both series (Fig. 3, A and B).

Are attractor dynamics observable at the start of a trial? The firing patterns in intermediate shapes might take time to reach the circle or square representation, when starting from more intermediate representations (see fig. S3, A and B). The firing patterns in successive 10-s intervals from the start of each trial were examined (18) in our largest dataset (17 remapped cells, see Fig. 4, A and B). Several results should be noted. First, the similarity of the firing patterns in square and circle probe trials to square and circle baselines is stable across intervals (with the possible exception of the very first interval in the square). Second, the firing in the squarelike octagons (1:7 and 2:6) is already more squarelike than circlelike in the first 10-s interval, but slowly becomes more squarelike over the following 2 min. A similar pattern is seen in one of the two more circlelike octagons (4:4). This result indicates a surprisingly slow component to attractor dynamics that should be studied further with larger samples of cells (a similar trend that did not reach significance was seen for our next-largest dataset, the eight remapped cells in fig. S2A).

Previous experiments, including our own, did not find the integrated cooperative behavior among pyramidal cells shown here (19–22). For example, the place cell representation initially adjusts continuously to changes in environmental shape alone, consistent with purely feed-forward processing (22, 23), and individual place cells slowly and independently learn to differentiate between square and circular environments made of the same material (17). One possibility is that synaptic modification in the CA3 recurrent collaterals is triggered by multimodal changes (e.g., of environmental shape, color, and texture) but not by unimodal changes, consistent with a hippocampal role in forming cross-modal associations between stimuli represented in disparate neocortical areas (7, 24). Greater remapping was also seen when both proximal and distal cues were changed than when either set was changed alone (25).

The results suggest the operation of both pattern separation, which creates radically different representations from highly similar environmental inputs, and coordination of large numbers of place cells to create a global maplike representation of each environment (2, 4, 5, 7, 10, 26). These functions are likely to originate in the hippocampus. Remapping has not been observed in its main cortical input, the entorhinal cortex (27, 28), and we expect cells there would respond incrementally to the gradual changes in the octagon series. Although our recordings were made in CA1, following previous authors (2, 4, 5, 7–9, 14), we hypothesize that pattern separation takes place in the dentate gyrus, whereas autoassociative integration takes place in the CA3 recurrent collaterals (see fig. S3C). Four

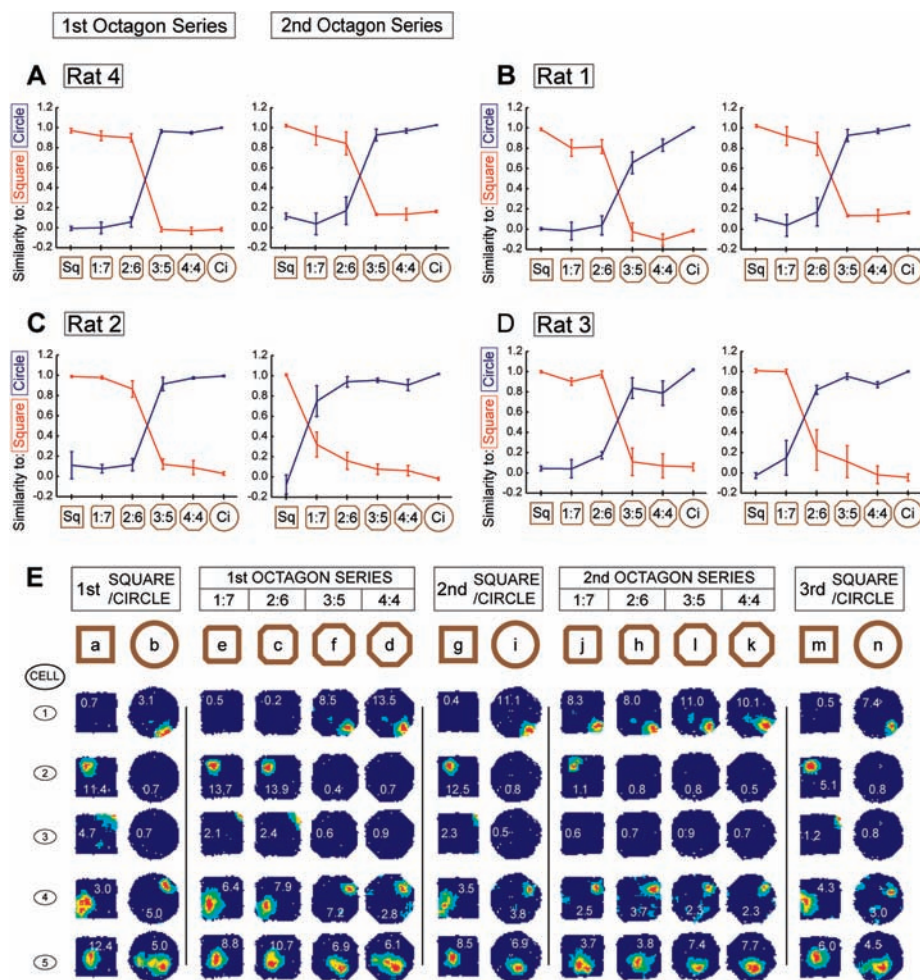


Fig. 3. Coordinated shift in square-to-circle switch point between the first and second octagon series. (A to D) Plots show the similarity of place cells' firing patterns in probe trials of varying shape to their firing patterns in square (red) or circle (blue) baseline trials [mean and SEM across cells (18)]. In the first series of octagons, all animals show abrupt remapping between the 2:6 and 3:5 octagons (A to D, left side); in the second series (right side), rats 4 (A) and 1 (B) again remap at this point, whereas rat 2 (C) remaps between the square and 1:7 octagon, and rat 3 (D) remaps between the 1:7 and 2:6 octagons. (E) Firing rate maps for all remapped cells for the two octagon series for rat 2.

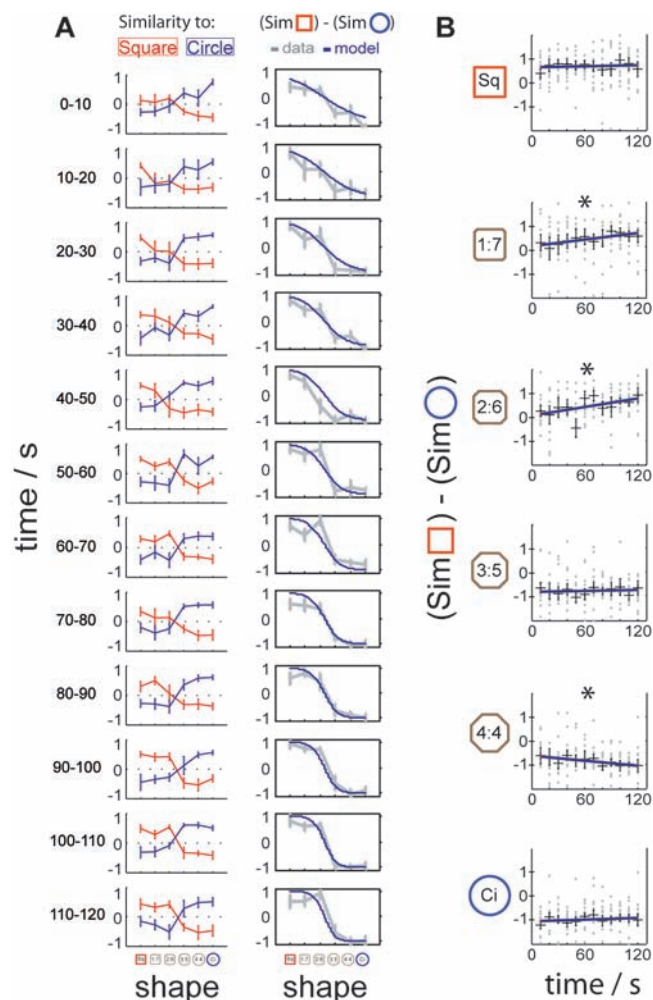


Fig. 4. Attractor dynamics of environmental representations. **(A)** Evolution of the firing pattern in successive 10-s intervals of trials in the different shaped environments. (Left column) The similarity of firing to that in square and circle baseline trials (mean and SEM for the 17 remapped cells in Fig. 2). (Right column) The difference in similarity of the firing pattern to square and circle baseline patterns. Gray line shows mean and SEM over cells of the difference between the red and blue curves shown in the left column. This becomes steadily more pronounced over time, and can be fitted by a sigmoid whose slope increases linearly with time (blue line: $y = 2 / (1 + \exp[(a_0 t + a_1] (s - s_0))) - 1$, where t is time in seconds, $s = 1$ to 6 corresponds to the series of shapes from square to circle, and $a_0 = 0.019$, $a_1 = 0.674$, $s_0 = 3.29$ were chosen to fit the data). **(B)** Firing patterns in intermediate 1:7 and 2:6 octagons become more squarelike over time, the patterns in 4:4 octagons become more circlelike, while the patterns in the square and circle remain unchanged (* $P < 0.05$ one-tailed, linear regression) (18).

References and Notes

1. D. O. Hebb, *The Organization of Behavior: A Neuro-psychological Theory* (Wiley, New York, 1949).
2. D. Marr, *Philos. Trans. R. Soc. Lond. B Biol. Sci.* **262**, 23 (1971).
3. J. J. Hopfield, *Proc. Natl. Acad. Sci. U.S.A.* **79**, 2554 (1982).
4. B. L. McNaughton, R. G. Morris, *Trends Neurosci.* **10**, 408 (1987).
5. A. Treves, E. T. Rolls, *Hippocampus* **2**, 189 (1992).
6. D. J. Amit, *Modelling Brain Function: The World of Attractor Neural Networks* (Cambridge Univ. Press, Cambridge, 1992).
7. J. L. McClelland, B. L. McNaughton, R. C. O'Reilly, *Psychol. Rev.* **102**, 419 (1995).
8. M. E. Hasselmo, B. P. Wyble, G. V. Wallenstein, *Hippocampus* **6**, 693 (1996).
9. K. I. Blum, L. F. Abbott, *Neural Comput.* **8**, 85 (1996).
10. J. O'Keefe, L. Nadel, *The Hippocampus as a Cognitive Map* (Oxford Univ. Press, Oxford, 1978); available at www.cognitivemap.net.
11. L. R. Squire, S. Zola-Morgan, *Trends Neurosci.* **11**, 170 (1988).
12. R. G. Phillips, J. E. LeDoux, *Behav. Neurosci.* **106**, 274 (1992).
13. H. Eichenbaum, *Nat. Rev. Neurosci.* **1**, 41 (2000).
14. K. Nakazawa et al., *Science* **297**, 211 (2002).
15. R. Muller, *Neuron* **17**, 813 (1996).
16. E. Bostock, R. U. Muller, J. L. Kubie, *Hippocampus* **1**, 193 (1991).
17. C. Lever, T. Will, F. Cacucci, N. Burgess, J. O'Keefe, *Nature* **416**, 90 (2002).
18. Materials and methods are available as supporting material on Science Online.
19. M. L. Shapiro, H. Tanila, H. Eichenbaum, *Hippocampus* **7**, 624 (1997).
20. S. Leutgeb, J. K. Leutgeb, A. Treves, M. B. Moser, E. I. Moser, *Science* **305**, 1295 (2004).
21. I. Lee, D. Yoganarasimha, G. Rao, J. J. Knierim, *Nature* **430**, 456 (2004).
22. J. O'Keefe, N. Burgess, *Nature* **381**, 425 (1996).
23. T. Hartley, N. Burgess, C. Lever, F. Cacucci, J. O'Keefe, *Hippocampus* **10**, 369 (2000).
24. P. Alvarez, L. R. Squire, *Proc. Natl. Acad. Sci. U.S.A.* **91**, 7041 (1994).
25. A. Vazdarjanova, J. F. Guzowski, *J. Neurosci.* **24**, 6489 (2004).
26. A. Samsonovich, B. L. McNaughton, *J. Neurosci.* **17**, 5900 (1997).
27. G. J. Quirk, R. U. Muller, J. L. Kubie, J. B. Ranck Jr., *J. Neurosci.* **12**, 1945 (1992).
28. M. Fyhn, T. Hafting, A. Treves, M. Moser, E. I. Moser, *Soc. Neurosci. Abstr.* **330.5** (2004).
29. J. K. Leutgeb et al., *Soc. Neurosci. Abstr.* **330.3** (2004).
30. S. Deneve, P. E. Latham, A. Pouget, *Nat. Neurosci.* **4**, 826 (2001).
31. R. U. Muller, M. Stead, J. Pach, *J. Gen. Physiol.* **107**, 663 (1996).
32. K. A. Norman, R. C. O'Reilly, *Psychol. Rev.* **110**, 611 (2003).
33. We thank S. Burton for technical assistance and T. Hartley for useful discussions. The work was supported by the Wellcome Trust and the Medical Research Council of the U.K.

Supporting Online Material

www.sciencemag.org/cgi/content/full/308/5723/873/DC1
 Materials and Methods
 Figs. S1 to S3
 References and Notes

20 December 2004; accepted 18 February 2005
 10.1126/science.1108905

examples are consistent with CA3's acting as an autoassociative network: the inability of mutant mice with disabled CA3 N-methyl-D-aspartate receptors to compensate for the removal of subsets of cues in the Morris water maze (14), the high sparsity of the CA3 representation (20, 25), signs of hysteresis within it (29), and the coherent response of CA3 place cells to inconsistent rotation of two sets of cues. CA3 place cells mainly followed proximal cues, whereas CA1 cells followed combinations of proximal and distal cues (21).

Our finding of coherent activity of place cells specific to each environment has several potential functional consequences. Such representations or "charts" (26) could serve to reduce interference between environments by providing orthogonal representations for each. They would also allow the firing of

large numbers of cells to be combined to provide an improved estimate of location (30). The capability for integrating information at distant locations with the representation of the current location may allow for short-cut and detour behavior (10, 31). More generally, attractor dynamics are thought to underlie context-dependent recollection [as opposed to, for example, familiarity-based recognition (32)]. Thus, understanding the creation of new attractors, and their dynamics, may directly inform the nature and function of "context" in context-dependent episodic memory and its failure in amnesia. Finally, the ability to study this mechanism at the single unit level allows for electrophysiological, pharmacological, and genetic investigation of the mnemonic function of the hippocampus in health and disease.

Note: This file was corrected on 10 May 2005, see page 4.

Science Supporting Online Material

Attractor Dynamics in the Hippocampal Representation of the Local Environment

Tom J. Wills,¹ Colin Lever,¹ Francesca Cacucci,¹ Neil Burgess,^{1,2} John O'Keefe^{1*}

¹Department of Anatomy and Developmental Biology, and ²Institute of Cognitive Neuroscience, University College London, London, WC1E 6BT, UK.

MATERIALS AND METHODS

Animals

Six Lister Hooded rats maintained on a 12:12 hour light:dark (lights off: 3 p.m.) schedule, weighing 280–380 g at time of surgery, were used as subjects.

Testing procedures

Experiments were conducted in a black-curtained, circular testing arena 2.5-m diameter. Rats were kept on a holding platform outside the arena before and after every trial. Testing environments were placed on a circular black platform 90 cm in diameter, which was cleaned before every trial. The centre of each testing environment had the same location relative to the curtained arena. An external white cue card (102 cm wide, 77 cm high) and standardized procedures for placing the rat into the box provided directional constancy throughout all trials. During trials the rat searched for grains of sweetened rice randomly thrown into the box about every 20 s. Two testing enclosures were used: a 'morph' box and a white wooden circle. The morph box (*S1*) is made from 32 pieces of rectangular cross-section plastic tubing, 7.5 cm wide, 50 cm high, held together on the inner surface by brown packing tape, covered with masking tape. It can be configured as a 79 cm diameter circle, a 62 cm sided square, and various octagons (see Fig. S1, a-d, for more details). The wooden circle measured 79 cm diameter, 50 cm high, with a smooth, painted, white inner surface. All trials were 10 minutes in duration, with 20 minute inter-trial intervals. Rats were trained with six trials per day: days 1-3, alternating morph square and white wooden circle; day 4, alternating square and circle, 2nd trial: white circle, 4th and 6th trial: morph circle; days 5-6: alternating morph square and morph circle. Octagon probe series was presented on day 7. (See Fig. S1, c and e, for details).

Cell recording

Methods of extracellular tetrode recording and analysis were as previously reported (*S1*, *S2*). Electrodes were moved into the CA1 pyramidal cell layer while rats sat on a holding platform in a different room. First exposure to the test environments occurred only after stable recording had been achieved, 2 to 4 weeks following surgery. Place units were isolated offline. Firing-rate maps were constructed by finding the number of spikes and the rat's dwell time in each 2 cm sided location bin, smoothing using a boxcar average over the 5 × 5 surrounding bins, and dividing the number of spikes by dwell time. They are shown as colour plots with each colour autoscaled to represent 20% of the peak rate (red to dark blue). Unvisited bins are shown in white. As previously (*S1*, *S2*), trials in which the firing rate fails to exceed 1.0 Hz are deemed not to express a spatial field and are shown as dark blue.

Data analysis

For comparison of firing rate maps from trials in different shaped boxes, corresponding bins in the different shapes were defined as those with the same direction from the centre and proportion of distance from the centre to the edge along that direction [a transformation that preserves the similarity of un-remapped fields (*SI*)], using nearest neighbour interpolation. Remapping was assessed using Pearson's r correlation over corresponding pairs of visited bins, excluding those with 0 Hz firing rate in both trials. A cell was considered stably *remapped* if the mean Square-Circle correlation was 0.5 less than the mean Square-Square and Circle-Circle correlation, i.e.:

$$\langle r \rangle_{sc} < \frac{1}{2}(\langle r \rangle_{ss} + \langle r \rangle_{cc}) - 0.5$$

where $\langle \rangle_{ss}$ indicates the average over all pairs of trials in Square boxes, $\langle \rangle_{cc}$ average over pairs of Circle trials, and $\langle \rangle_{sc}$ average over pairs of trials, one in each shape. Stable remapping over the 3 Square and Circle baselines (which span the probe trials-see below) is important to prevent temporal instability being confounded with effects of probe shape.

For remapped cells, the similarity of the firing pattern in a given shape I to that in the 3 Square baseline trials, relative to its similarity to that in the 3 Circle baseline trials, is defined as:

$$s(I, S) = (\langle r \rangle_{is} - \langle r \rangle_{sc}) / (\langle r \rangle_{ss} - \langle r \rangle_{sc})$$

where $\langle \rangle_{is}$ is the average over pairs of trials, one in shape I and one in the Square. A value of 1.0 indicates a firing pattern identical to that in the Square, a value of 0.0 indicates firing as different to that in the Square as the firing in the Circle is. Similarly, we define the similarity of firing in shape I to that in the Circle, relative to that in the Square as:

$$s(I, C) = (\langle r \rangle_{ic} - \langle r \rangle_{sc}) / (\langle r \rangle_{cc} - \langle r \rangle_{sc}).$$

Both similarity measures are necessary, because lack of similarity to the Square does not necessarily imply similarity to the Circle, and vice versa. These measures work well when a field is expressed in both shapes, or in one shape but not the other, but they do not reliably reflect similarity in pairs of low-rate shapes (i.e., both < 1.0 Hz). In this case we replace correlation coefficients with peak-rate similarity:

$$R(A,B) = \min(\text{peak rate A, peak rate B}) / \text{mean}(\text{peak rate A, peak rate B})$$

(this measure behaves similarly to r for rate-remapped cells for trials with > 1 Hz peak rate, is more stable for trials with < 1 Hz peak rates, but does not capture field position remapping), so that the similarity to Square measure becomes:

$$s(I, S) = (\langle R \rangle_{is} - \langle R \rangle_{sc}) / (\langle R \rangle_{ss} - \langle R \rangle_{sc})$$

and likewise for similarity to Circle.

For analysis of 10-s intervals (Fig. 4, A and B), the similarity measure is applied as above, using the firing rate map derived from the 10-s interval for trial I and the full duration rate maps for baseline trials S and C (two 10-s interval maps do not contain sufficient pairs of mutually visited bins for meaningful correlations), and the correlation r is used in all cases (peak-rate similarity R cannot be used as the animal does not adequately sample the environment in 10-s, often missing the centre of the place field).

Cells that fired no spikes in the given intervals for a given shape are omitted from the similarity data for that interval and shape. Note that the similarity of a 10-s interval in the Square to Square baselines is less than 1.0 (and its similarity to Circle baselines less than 0.0) due to the greater noise in these maps than in full duration maps. Linear regression was performed on the difference in similarity to square and circle baselines, i.e.: $s(I, S) - s(I, C)$, of the individual cells.

Note: This file was corrected on 10 May 2005 to change lights on to lights off at 3 p.m. in the first line of text and to correct two equations within the legend to Fig. 3. The originally posted version is available [here](#).

SUPPORTING FIGURE 1

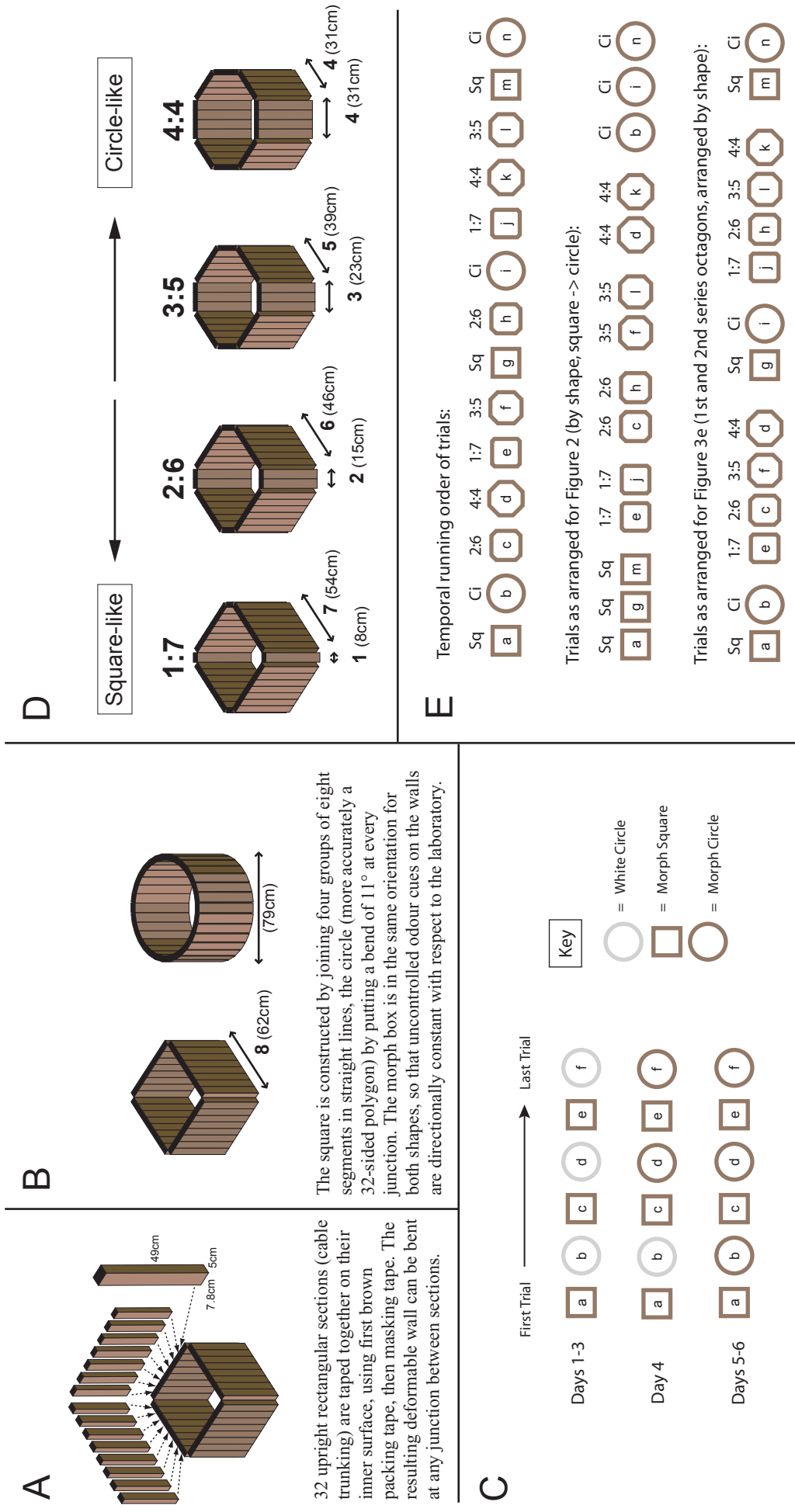


Fig. S1. Methods for Rapid Remapping and Octagon Probe experiments. **A**) Construction of morph box. **B**) Morph box configured as square and circle. **C**) Protocol for rapid remapping training. Colour of outline shapes indicate type of material, see key for details. Letters inside shapes indicate temporal order of trials. All trials 10 mins, inter-trial interval 20 mins. **D**) Morph box configured as intermediate octagons, for octagon probe trials. Octagons incrementally intermediate between square and circle are constructed by changing the relative lengths of adjacent sides. All internal angles are always 135°. These shapes are labelled according to the number of morph box sections that make up the adjacent sides. **E**) Protocol for Octagon Probe Trials. Top row: trials in actual running order. Letters inside shape indicate temporal order of trials. All environments constructed using morph box. All trials 10 mins, inter-trial interval 20 mins. Middle and bottom rows: order of trials rearranged to match presentation in figures 2 (middle), 3E (bottom).

SUPPORTING FIGURE 2

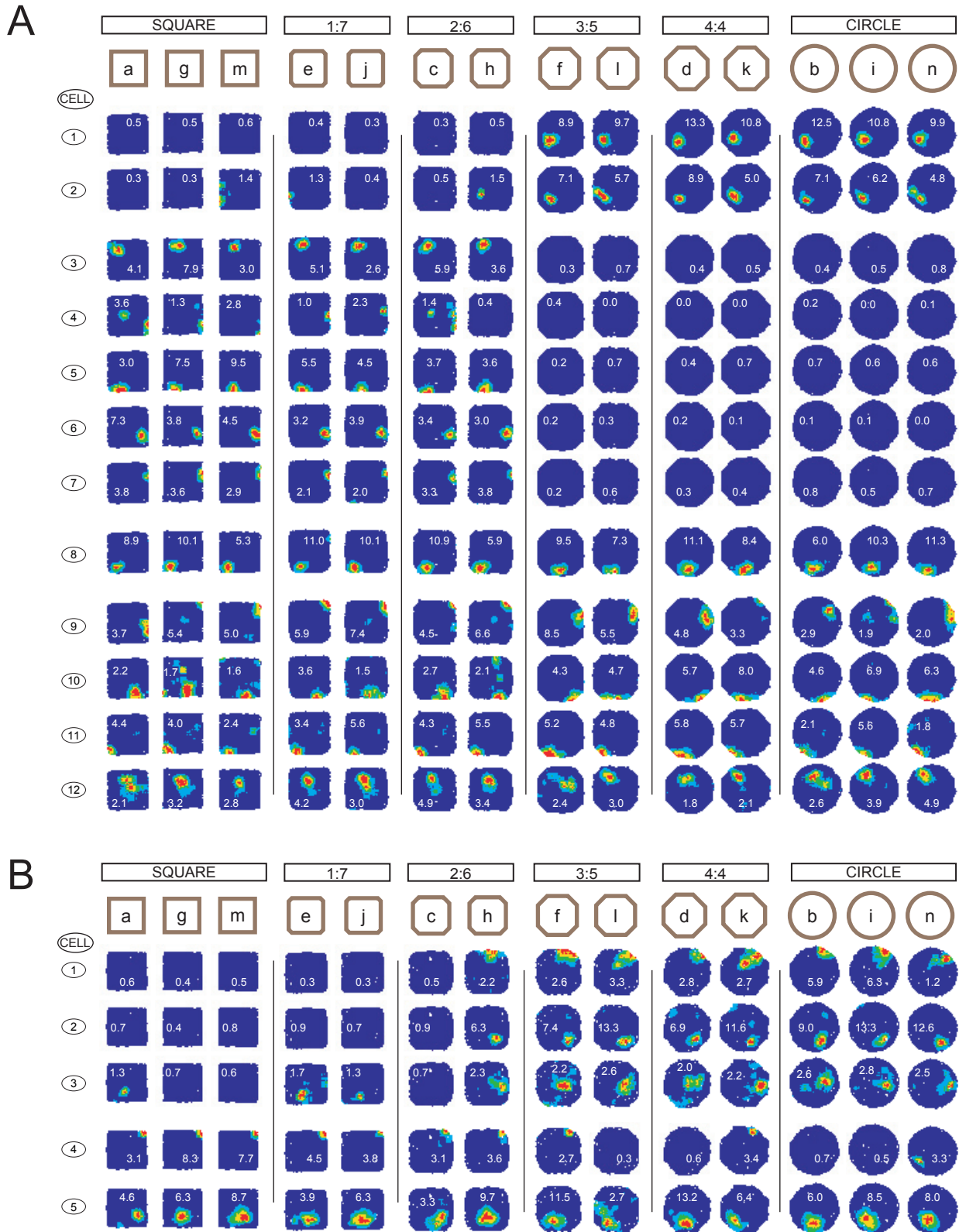


Fig. S2. Abrupt and coherent remapping between square-like and circle-like representations during intermediate octagonal environments. Layout of maps as for fig. 2. (A) Rat 1. Cells 1-8 switch from square-like to circle-like representations between 2:6 and 3:5 octagons on both 1st and 2nd series. Cells 9-12 did not reach our criterion for remapping. (B) Rat 3. Cells 1-3 switch representations between 2:6 and 3:5 octagons on the first series, and between 1:7 and 2:6 octagons on the second series. Cells 4-5 did not reach our criterion for remapping. See Materials and Methods for details.

SUPPORTING FIGURE 3

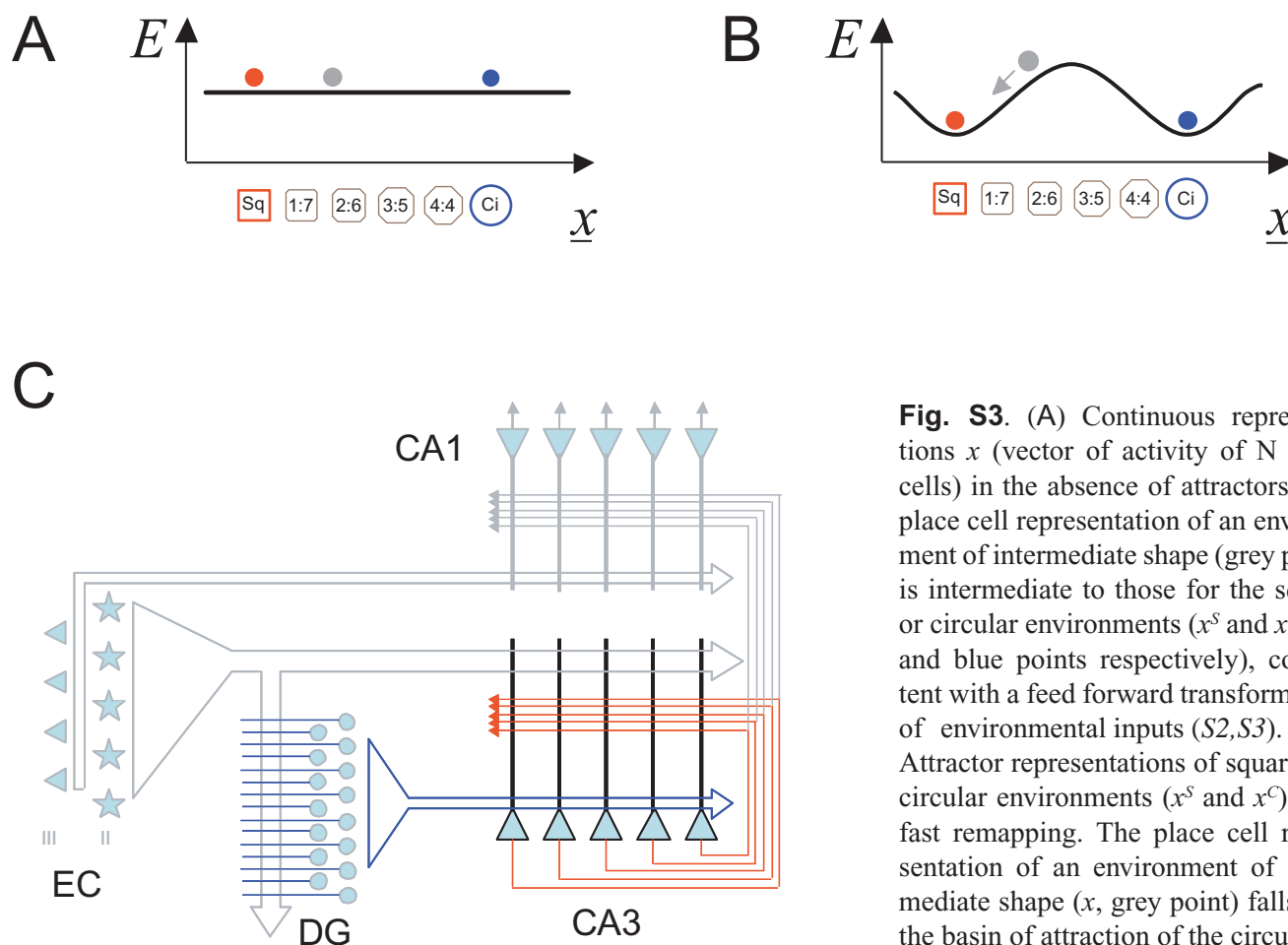


Fig. S3. (A) Continuous representations x (vector of activity of N place cells) in the absence of attractors. The place cell representation of an environment of intermediate shape (grey point) is intermediate to those for the square or circular environments (x^S and x^C , red and blue points respectively), consistent with a feed forward transformation of environmental inputs ($S2, S3$). (B) Attractor representations of square and circular environments (x^S and x^C) after fast remapping. The place cell representation of an environment of intermediate shape (x , grey point) falls into the basin of attraction of the circular or square representation and converges onto that representation over time (grey arrow). This behaviour could result from modification of recurrent connections between place cells. In one of the simplest models ($S4$), activity of cell i is

modelled as $x_i = \pm 1$. Connections between cells i and j are symmetric, with synaptic 'weight' $w_{ij} = w_{ji}$. The dynamics of the system are given by: $x_i(t+1) = \text{sign}(\sum_j w_{ij} x_j(t))$, such that the 'energy' or Lyapunov function of the system: $E \propto -\sum_{ij} w_{ij} x_i x_j$, can only reduce. If connection weights undergo a form of Hebbian learning during representations x^S and x^C (such that $w_{ij} \propto \sum_{\mu=S,C} x_i^\mu x_j^\mu$) then these representations become attractors: similar enough representations to x^S or x^C converge onto that representation. Similar behaviour is also shown by more biologically realistic models ($S5-S8$). (C) Postulated functional anatomy of the hippocampus ($S6, S7, S9-S13$). The pathway from entorhinal cortex (EC) to CA3 drives the place cell representation. Remapping (blue connections): The large number of cells in the dentate gyrus (DG) allows pattern separation of the EC input, with plasticity in the EC-DG pathway causing remapping. The powerful and selective DG-CA3 pathway imposes new representations in CA3, with plasticity in the EC-CA3 pathway allowing the EC input to drive the new representation. Attractors (red connections): The dense recurrent connections between CA3 pyramidal cells mediate an attractor or auto-associative network in CA3: plasticity in these connections allows a representation to become an attractor. The attractor-mediated CA3 representation drives the CA1 representation via the CA3-CA1 pathway, and could be compared to the EC representation via the projection from small pyramidal cells in EC layer III.

References and Notes

- S1. C. Lever, T. Wills, F. Cacucci, N. Burgess, J. O'Keefe, *Nature* **416**, 90 (2002).
- S2. J. O'Keefe and N. Burgess, *Nature* **381**, 425 (1996).
- S3. T. Hartley, N. Burgess, C. Lever, F. Cacucci, J. O'Keefe, *Hippocampus* **10**, 369 (2000).
- S4. J. J. Hopfield, *Proc.Natl.Acad.Sci.U.S.A* **79**, 2554 (1982).
- S5. D. J. Amit, *Modelling Brain Function: The World of Attractor Neural Networks* (Cambridge University Press, Cambridge, 1992).
- S6. A. Treves and E. T. Rolls, *Hippocampus* **2**, 189 (1992).
- S7. J. L. McClelland, B. L. McNaughton, R. C. O'Reilly, *Psychol.Rev.* **102**, 419 (1995).
- S8. A. Samsonovich and B. L. McNaughton, *J. Neurosci.* **17**, 5900 (1997).
- S9. D. Marr, *Philos. Trans. R. Soc. Lond. B Biol. Sci.* **262**, 23 (1971).
- S10. B. L. McNaughton and R. G. Morris, *Trends Neurosci.* **10**, 408 (1987).
- S11. K. Nakazawa et al., *Science* **297**, 211 (2002).
- S12. M. E. Hasselmo, B. P. Wyble, G. V. Wallenstein, *Hippocampus* **6**, 693 (1996).
- S13. K. I. Blum and L. F. Abbott, *Neural Comput.* **8**, 85 (1996).